World Scientific
www.worldscientific.com

STOCHASTIC RESONANCE IN HAIR CELL MECHANOELECTRICAL TRANSDUCTION

MATTHEW BENNETT and KURT WIESENFELD

Center for Nonlinear Science and School of Physics
Georgia Institute of Technology, Atlanta, GA 30030

FERNAN JARAMILLO

Department of Biology
Carleton College, Northfield, MN 55057

Hair cells are the mechanoelectrical transducers in the auditory system of many species, including humans. Experiments show that transduction in individual hair cells displays stochastic resonance, with optimum response at the natural noise level of living cells. We find that many of the observed features are captured by a simple version of a physiologically faithful model of the transduction mechanism. These findings may resolve a longstanding puzzle in evolutionary biology concerning the structure of the cochlea.

Keywords: Brownian motion; cochlea; hearing; transduction; hair bundle.

1. Introduction

Stochastic resonance is a phenomenon where the output coherence of a nonlinear system (a detector, perhaps) is optimized only in the presence of some finite level of input noise. The study of stochastic resonance is by now a mature field [1–5]. A great many systems show the effect, and while some fundamental issues remain open by and large theory is in good agreement with experiment. The biggest unresolved question is whether there are any practical applications of stochastic resonance.

The suggestion that stochastic resonance plays a role in biology was made at least as early as 1991 [6–8]. Sensory neurons are notoriously noisy, and stochastic resonance might account for the exquisite sensitivity of some animals to detect weak coherent signals. In 1993, Moss *et al.* published experiments on the mechanoreceptor hair cells of crayfish [9]. Two years later, Bezrukov and Vodyanoy reported data showing stochastic resonance at the subcellular level [10]. Other examples were found in rapid succession including experiments on the cercal system of crickets [11] and in mammalian cutaneous tissue [12], among others [13].

But does stochastic resonance actually play a functional biological role? Moss *et al.* [14, 15] have shown how electrical noise improves the ability of paddlefish to find food. The search for stochastic resonance in higher order functions has led to studies in vision [16], balance [17], respiration [18], and hearing [19].

In this paper, we address the possible beneficial role of noise in the auditory system. Experiments have shown that hair cells, which act as a primary mechano-electrical transducer in many animals (including humans), exhibit stochastic resonance at physiologically relevant noise levels [20–22]. Nanometer-sized fluctuations in the bundle position comparable to those due to equilibrium Brownian motion [23] resulted in a clear increase in the cell's response to a weak periodic stimulus. We explore this effect using a model based on the gating spring picture of mechanoelectrical transduction [25]. The hair cell is in many ways an ideal testbed for studying stochastic resonance in a biological setting, since (i) much of the hair cell physiology is known in detail and (ii) the physics involved is purely mechanical.

Mammalian auditory hair cells reside in the organ of Corti, within the scala media of the Cochlea (Fig. 1). Within this organ there is an evident division of labor between the majority outer hair cells (OHCs), and the single row of inner hair cells (IHCs). The former have their hair bundles embedded in the overlying tectorial membrane which in response to auditory stimulation acts to deflect them. These OHCs, which are motile, are thought to actively amplify and refine the local motion of the organ of Corti that also drives the inner hair cells. In contrast, IHCs, which are incapable of this active motility, convey most of the afferent information that goes to the brain. They are viewed, therefore, as the main auditory system detector. There is no evidence that the bundles of IHCs are embedded in the tectorial membrane (they are thought to be driven by fluid motion), and therefore they could undergo significant Brownian motion. It might seem reasonable to assume that directly driving the IHCs by the overlying tectorial membrane, a modus operandi also employed by all the other non-auditory hair cell organs, would be most effective. Why then, has the main detector in the auditory system become uncoupled from the structure most capable of driving it? What is the selective advantage of this modification in the evolutionary history of the auditory system? We return to this question in the discussion.
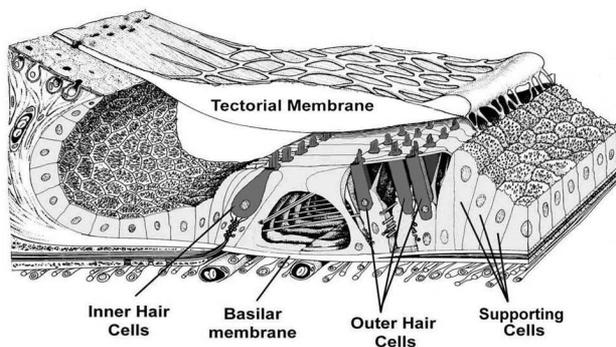

Fig. 1. The organ of Corti. From Ref. [24].

2. Background

The auditory system is a marvelous performer in a noisy world [25, 26]. In the frequency midrange (2–4 kHz) a person can detect sounds with a peak sound pressure of 20 μPa, an amount close to the change in atmospheric pressure we experience with a change in elevation of 1.9 μm. A threshold auditory stimulus corresponds to an eardrum motion of about one tenth of an Angstrom. Because this is approximately equal to the motions resulting from the random collisions of air molecules against the eardrum, it has been the traditional view that noise limits the sensitivity of the auditory system. But this is almost certainly wrong. If we look at the level of the hair cell, rather than the eardrum, we see that the cells successfully transduce mechanical displacements some 30 times smaller than the hair bundle's root-mean-square Brownian motion caused by molecular collisions with the ambient fluid. Experiments show that hair cells exhibit stochastic resonance, suggesting that bundle fluctuations could be a useful influence rather than a harmful one [20–22,27]. Importantly the effects occur at biologically relevant noise levels, for hair bundle fluctuations of about 2 or 3 nanometers [23].

How can we explain the positive effects of mechanical noise on mechanoelectrical transduction? Let's begin by considering the hair cell transduction apparatus: each hair cell is equipped with a single hair bundle, comprising several dozen specialized processes named stereocilia (referred to in our model as rods). Fig. 2 shows a detail of an IHC's characteristic bundle (left panel). Although details vary from species to species, in humans a typical bundle consists of 60 stereocilia arranged in an array of three ranks, each with 20 stereocilia. Although fine filaments connect stereocilia to each other at different points, the tip link is the only element which is aligned with the axis of mechanical sensitivity of the hair cell, and its destruction abolishes mechanoelectrical transduction. Each stereocilium is attached to its taller neighbor via a tip link (shown in middle and right panels of Fig. 2) which at least at one extreme is coupled to the gate of an ion channel whose opening and closing it controls. The gate of the ion channel, which swings about 2 nm to open, fluctuates between two distinct states (closed and open). If the gate is open, cations may flow through the ion channel, depolarizing the hair cell and causing it to release its neurotransmitter.

Because the response of the hair bundle is essentially mechanical it is straightforward to model. The key element in the transduction process is the effect of the tip link on the gate. Figure 3 is a schematic of our basic model. Two rods are connected by an elastic element (the tip link). The bottom of each rod is fixed to the cell membrane and pivots about this point in the plane of the drawing. The inset shows how the tip link is connected to a gate on the longer rod. As depicted in the figure, we assume the gate is fixed at one end so that it rotates in the same plane as the rod.

The potential energy for the system may be written

$$U(\theta_1, \theta_2, \phi) = U_{el}(\theta_1, \theta_2, \phi) + U_{con}(\phi) \qquad (1)$$

where θ_1, θ_2, ϕ are the angular displacements of the long rod, short rod, and gate, respectively. The first term is the elastic potential energy (stored in the base torsion springs and the tip link); the second term is the conformational potential energy
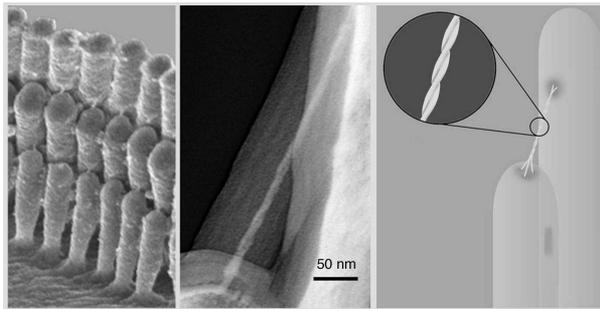
Fig. 2. The tip link and mechanoelectrical transduction. Left: A scanning electron micrograph shows the typical three-rank organization of the inner hair cell hair bundle in mammals. Middle: A deep freeze-etch image reveals the thin tip link joining the tips of two adjacent stereocilia (the thick halo around the tip link is caused by the carbon coating used to prepare the sample. Right: A model of the tip link structure. Tip links seem to branch near their extremes. It is not known how many of these branches are coupled to the gate of the transduction channels. Courtesy of Dr. Bechara Kachar, NIH.
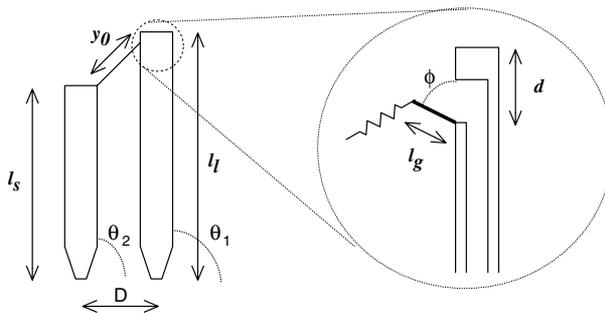

Fig. 3. Schematic of the two-rod one-gate model. The inset shows the connection between the elastic tip link and the gate.

of the gate. In "the wild", a stimulus (pressure wave) exerts a body force on the rods, which pivot about their bases. This stretches the tip link and thus affects U_{el}, which in turn alters the switching behavior of the gate.

Motivated by the experiments of Ref. [20], we consider a constrained version of the model where the rod positions are directly controlled, i.e. θ_1 and θ_2 are prescribed functions of time. Since the gate behaves to good approximation as a two state system – the conductance of a single gate randomly switches between two fixed levels – we use a thermal activation rate description [25]. The probability p that the gate is open evolves according to

$$\dot{p} = -(r_c + r_o)p + r_c \qquad (2)$$

where r_c is the transition rate out of the closed state, and r_o is the transition rate out of the open state. The rates have the form

$$r_c = f_c \exp\left(-\Delta U_c/kT\right) \qquad (3)$$
$$r_o = f_o \exp\left(-\Delta U_o/kT\right) \qquad (4)$$

where ΔU_c and ΔU_o are the potential energy barriers in the closed and open states, respectively; f_c, f_o are the attempt frequencies; k is Boltzman's constant; and T is the temperature.

Since we want to study the situation where the rates are time dependent (owing to the motion of the hair bundle), the reduction to a rate-equation description assumes a separation of time scales: the rates must be slowly varying with respect to the intrawell relaxation. We expect this to be true in our problem: the individual opening/closing events of the gate are much faster than the motion of the rod. Whereas the sensitivity of our hearing is centered in the low kilohertz range (with sub-millisecond periods of hair bundle oscillation) the individual transitions of ion channel gates are usually too fast to be resolved, and are generally thought to be in the sub-microsecond range [30].

3.   Determining the Model Parameters

The governing equation (2) requires setting the transition rates r_c and r_o, which depend on the instantaneous position of the rods and gate through the elastic energy stored in the tip link. This in turn depends on the following parameters: K is the tip link spring constant; y_0 is the unstretched length of the tip link; D is the distance between the bases of the two rods; ℓ_ℓ is the distance from the base of the long rod up to the gate hinge; ℓ_g is the length of the gate; and ℓ_s is the length of the short rod. In addition to these, we need to specify the three extremal values of the conformational potential energy U_{con}: U_c is the energy when the gate is closed, U_o when it is open, and U_b when the gate is in the intermediate "activated" position. (In terms of the quantities introduced above, $\Delta U_o = U_b - U_o$ in the absence of the tiplink energy, and similarly $\Delta U_c = U_b - U_c$.) Finally, we take the rod deflections to be equal and prescribed:

$$\theta = A + B \sin \omega t + C \xi(t) \tag{5}$$

where A, B, and C are constants and ξ is a dimensionless noise with zero mean and unit variance. The sinusoidal term is meant to mimic the body force due to a pure tone.

We want to study the effect of noise under biologically relevant circumstances, rather than just testing whether stochastic resonance (for example) can occur in principle. Although our model depends on several parameters, the physiology is sufficiently well known that most are known from direct measurements. Even so, precise values are not available for all of the parameters and in fact they vary substantially from one species to another. We can divide the various parameters into three groups. The first group consists of quantities which are readily determined from direct imaging of the hair bundle; the second group can be set by comparison with static measurements of the hair bundle; the third group may be fixed by comparison with transient response measurements.

The parameters that can be set from imaging are the rod lengths ℓ_ℓ and ℓ_s and their separation D. Typical values are (for example, for the bullfrog):

$$\ell_\ell = 8500 \; nm \,; \quad \ell_s = 6125 \; nm \,; \quad D = 940 \; nm \,.$$

Next in the static response measurements, the bundle tip (upper end of the long rod) is displaced a fixed distance X from its equilibrium value, and the steady state
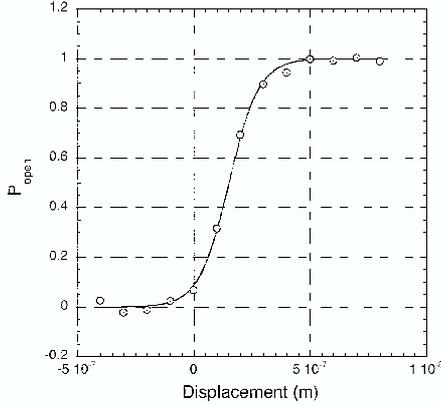
Fig. 4. Experimental data of P_{open} vs. X, with the theoretical prediction superimposed. Courtesy of Dr. Peter Gillespie.

probability that the gate is opened is measured. (X is positive for a deflection to the right in Fig. 3.) Such a P_{open} vs. X is shown in Fig. 4. For this situation, we can get an explicit formula for P_{open} by setting $dp/dt = 0$ in Eq. (2), so that

$$P_{open}^{-1} = 1 + \exp\left[\left(\Delta U_c - \Delta U_o\right)/kT\right]. \tag{6}$$

This expression is also plotted in Fig. 4. We pick three features of the experimental curve to use for fitting the model parameters: the value of P_{open} when no stimulus is applied (and so $X = 0$), the value of X at which $P_{open} = 1/2$, and the overall width of the curve. From these we determine values for K, y_0, and the difference $U_o - U_c$:

$$K = 1257~\mu N/nm\,;\quad y_0 = 975~nm\,;\quad U_o - U_c = 5.73 \times 10^{-21}~J\,.$$

To get an idea of the scale of this energy difference, it is about $1.4kT$ at room temperature.

Turning to the transient relaxation experiment, the system is first allowed to come to static equilibrium with the bundle tip at some value $X = X_1$. Then, X is suddenly changed to a new value X_2, and the time evolution of P_{open} is measured. From Eq. (2), the predicted response is

$$p(t) = [p(0) - p(\infty)]\,e^{-\lambda t} + p(\infty) \tag{7}$$

where $p(0)$ and $p(\infty)$ are the steady state values given by Eq. (6) for X_1 and X_2, respectively, and the relaxation rate is $\lambda = r_c + r_o$ evaluated for X_2. From λ, the quantity U_b follows via:

$$U_b = kT \ln\left[f_c \exp(U_c/kT) + f_o \exp(U_o/kT)\right] - kT \ln \lambda\,.$$

The one parameter not yet fixed is the gate length ℓ_g. This number is variously estimated as being about 2 to 4 nanometers [25]. In what follows, we set $\ell_g = 2.0$ nm.

4.   Effect of Noise on Model's Behavior

First we consider the behavior with a periodic stimulus and no bundle noise, and look at the dependence of the output as a function of temperature. In the two state approximation considered here, the gate switches between open and closed positions; the transduced current likewise switches between on and off levels. For either quantity the output power spectrum is the sum of a broad background and a narrow spike at the signal frequency. Dividing the area under the narrow spike by the broadband power in an equal bandwidth at nearby frequencies yields the signal to noise ratio (SNR). If we set the dc stimulus A at the value for which $P_{open} = 0.5$, we recover (to good approximation) the symmetric situation analyzed in Ref. [29], and can apply those results directly. The broad curve in the left panel of Fig. 5 is a plot of SNR vs. T using the rate formulas (4) with $f_o = f_c = kT/h$, a common choice in studies of gate dynamics [25]. The SNR peaks at about 5600° Kelvin, which is absurdly high from a biological perspective (and is, literally, an astronomically high temperature).

This high temperature may be an artifact of the rate formula. A more accurate choice is the Kramers formula [28]; the drawback is that this introduces three new parameters (namely, the curvature of conformational potential energy at the open, barrier, and closed positions). To set these parameters requires more information than is currently available. In the meantime, a simple compromise is to keep $f_o = f_c$ but treat this as a single free parameter f. Adjusting f can bring down the SNR peak substantially. This is shown in the left panel of Fig. 5 by the narrow curve; the right panel shows a close-up. Note that if we treat f as a free parameter it is no longer a function of T, so it is necessary to recalibrate the other system parameters.

We now turn to the case at fixed temperature and with bundle fluctuations included, which introduces a second noise source in the gate dynamics. At present an adequate theory for this situation is lacking, but we can see how a plot of SNR vs. bundle noise will look. An increase in bundle fluctuations qualitatively corresponds to moving along the increasing-T axis in Fig. 5. If we choose a value of f such that the ambient temperature lies a bit below the SNR peak, we get a curve very similar to those seen in the hair cell experiments, which show a maximum increase in SNR by about a factor of two.
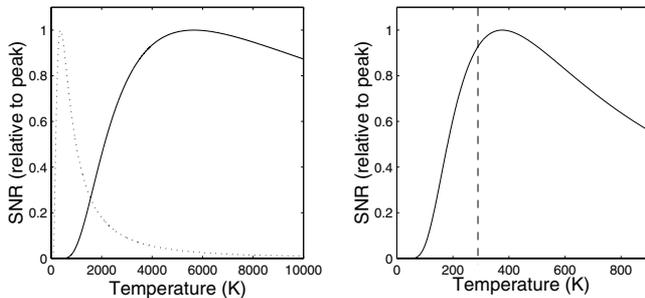

Fig. 5. Output SNR vs. temperature in degrees Kelvin with no bundle fluctuations. Left: The broad curve uses $f_o = f_c = kT/h$ in the rate formula (4); the narrow curve uses $f = 1.2 \times 10^6 \, s^{-1}$. Right: Close-up of dashed curve at left, with vertical line at $T = 298$ degrees.

A quantitative connection between bundle noise and predicted SNR requires extending the theory. One possibility is to stay within the framework of two state rate theory, and treat the transition rates as having a random component. This idea was originally applied to stochastic resonance by Bezrukov and Vodynoy and might be extended to apply to our situation [31]. An alternative approach is to view the two (physically uncorrelated) noise sources as comprising a single source characterized by an effective temperature, allowing one to map the problem back onto standard two state theories of stochastic resonance. This approach seems feasible in the limit of fast bundle fluctuations [32].

5.   Discussion

The gating spring picture of hair cells was previously known to be a good description of transduction behavior under static conditions. We have extended the model to include dynamical and even stochastic motion of the hair bundle. As in experiments, the addition of bundle noise leads to an improvement in the output signal to noise ratio, by a modest but biologically significant amount. This lends support to the hypothesis that noise plays a functional role in hearing.

We close by returning to the evolutionary puzzle described in the introduction. The rationale for the uncoupling of IHCs bundles from the tectorial membrane is that it may allow these cells to use noise to improve the detection of very weak signals. Outer hair cells, whose hair bundles are restrained by their attachment to the tectorial membrane, serve to detect stronger signals and to locally amplify the auditory stimulus. If this hypothesis is correct, the addition of bundle noise should degrade the SNR in the presence of strong signals. Indeed, this is just what one finds in the two-state model [5]. Such behavior is well known in conventional stochastic resonance settings: for large input signals, the SNR is a monotonically decreasing function of the noise amplitude. Experiments on hair cells likewise show monotonic degradation for large signals [22].

It is worth noting that in other contexts noise can play a beneficial role in the presence of strong signals [33]. Such supra-threshold stochastic resonance can occur when effects of mechanical inertia are significant, a fact which has important consequences, for example, in the design of cochlear implants [34].

Acknowledgements

References

[1] F. Moss, *Stochastic Resonance: from ice ages to the monkey's ear*, in Contemporary Problems in Statistical Physics, ed. G. H. Weiss, SIAM, Philadelphia (1994) 205–253.

[2] K. Wiesenfeld and F. Moss, *Stochastic resonance and the benefits of noise: from ice ages to crayfish and SQUIDs*, Nature **373** (1995) 33–36.

[3] M. I. Dykman, D. G. Luchinsky, R. Mannella, P. V. E. McClintock, N. D. Stein and N. G. Stocks, *Stochastic resonance in perspective*, Nuovo Cimento D **17** (1995) 661–683.

[4] A. Bulsara and L. Gammaitoni, *Tuning in to noise*, *Phys. Today* **49** (1996) 39–45.

[5] L. Gammaitoni, P. Hanggi, P. Jung and F. Marchesoni, *Stochastic resonance*, *Rev. Mod. Phys.* **70** (1998) 223–287.

[6] A. Longtin, A. Bulsara and F. Moss, *Time-interval sequences in bistable systems and the noise-induced transmission of information by sensory neurons*, *Phys. Rev. Lett.* **67** (1991) 656–659.

[7] A. Bulsara, E. W. Jacobs, T. Zhou, F. Moss and L. Kiss, *Stochastic resonance in a single neuron model: Theory and anlaog simulation*, *J. Theor. Biol.* **152** (1991) 531–556.

[8] D. R. Chialvo and A. V. Apkarian, *Modulated noisy biological dynamics. Three examples*, *J. Stat. Phys.* **70** (1993) 375–391.

[9] J. K. Douglass, L. Wilkens, E. Pantazelou and F. Moss, *Noise enhancement of information transfer in crayfish mechanoreceptors by stochastic resonance*, *Nature* **365** (1993) 337–340.

[10] S. M. Bezrukov and I. Vodyanoy, *Noise-induced enhancement of signal transduction across voltage-dependent ion channels*, *Nature* **378** (1995) 362–364.

[11] J. Levin and J. Miller, *Broadband neural encoding in the cricket cercal sensory system*, *Nature* **380** (1996) 165–168.

[12] J. Collins, T. Imhoff and P. Grigg, *Noise-enhanced information transmission in rat SA1 cutaneous mechanoreceptors via aperiodic stochastic resonance*, *J. Neurophysiology* **76** (1996) 642–645.

[13] R. D. Astumian and F. Moss, guest editors, *Focus issue*: *The constructive role of noise in fluctuation driven transport and stochastic resonance*, *Chaos* **8** (1998) 533–736.

[14] D. F. Russell, L. Wilkens and F. Moss, *Use of behavioral stochastic resonance by paddlefish for feeding*, *Nature* **402** (1999) 219–223.

[15] J. Freund, L. Schimansky-Geier, B. Beisner, A. Neiman, D. F. Russell, T. Yakusheva and F. Moss, *Behavioral stochastic resonance*: *How the noise from a Daphnia swarm enhances individual prey capture by juvenile paddlefish*, *J. Theor. Biol.* **214** (2002) 71–83.

[16] T. Mori and S. Kai, *Noise-induced entrainment and stochastic resonance in human brain waves*, *Phys. Rev. Lett.* **88** (2002) 218101/1–4.

[17] A. Priplata, J. Niemi, J. Harry, L. Lipsitz and J. Collins, *Vibrating insoles and balance control in elderly people, Lancet* **362** (2003) 1123–1124; A. Priplata, J. Niemi, M. Salen, J. Harry, L. Lipsitz and J. Collins, *Noise-enhanced human balance control*, *Phys. Rev. Lett.* **89** (2002) 238101/1–4.

[18] I. Hidaka, D. Nozaki and Y. Yamamoto, *Functional stochastic resonance in the human brain*: *Noise induced sensitization of baroreflex system*, *Phys. Rev. Lett.* **85** (2000) 3740–3743.

[19] R. Morse and E. Evans, *An information theoretic approach to cochlear implant coding*, *Nat. Med.* **2** (1996) 928–932; R. Morse, D. Allington and N. Stocks, *AIP Conf. Proc.* **665** (2003) 125–132, and references therein.

[20] F. Jaramillo and K. Wiesenfeld, *Mechanoelectrical transduction assisted by Brownian motion: A role for noise in the auditory system*, *Nature Neuro.* **1** (1998) 384–388.

[21] F. Jaramillo and K. Wiesenfeld, *Physiological noise level enhances mechanoelectrical transduction in hair cells*, *Chaos, Solitons and Fractals* **11** (2000) 1869–1874.

[22] A. Indresano, J. Frank, P. Middleton and F. Jaramillo, *Mechanical Noise Enhances Signal Transmission in the Bullfrog Sacculus*, *J. Assoc. Res. Otolaryngol.* **4** (2003) 363–370.

[23] W. Svrcek-Seiler, I. Gebeshuber, F. Rattay, R. Biro and H. Markum, *Micromechanical models for the Brownian motion of hair cell stereocilia*, *J. Theor. Biol.* **193** (1998) 623–630.

[24] Figure reprinted from D. J. Lim, *Functional structure of the organ of Corti: a review*, *Hearing Research* **22** (1986) 117–146.

[25] J. Howard, W. M. Roberts and A. J. Hudspeth, *Mechanoelectrical transduction by hair cells*, *Ann. Rev. Biophys. Chem.* **17** (1988) 99–124.

[26] K. Wiesenfeld and F. Jaramillo, *Minireview of stochastic resonance*, *Chaos* **8** (1998) 539–548.

[27] K. R. Henry, *Noise improves transfer of near-threshold, phase-locked activity of the cochlear nerve: Evidence for stochastic resonance? J. Comparative Physiol. A* **184** (1999) 577–584.

[28] C. Gardiner, *Handbook of Stochastic Methods for Physics, Chemistry, and the Natural Sciences*, Springer, Berlin (1983).

[29] B. McNamara and K. Wiesenfeld, *Theory of stochastic resonance*, *Phys. Rev. A* **39** (1989) 4854–4869.

[30] B. Sakmann and E. Neher, *Single-Channel Recording*, Plenum Press, New York (1995).

[31] S. Bezrukov and I. Vodyanoy, *Stochastic resonance in nondynamical systems without response thresholds*, *Nature* **385** (1997) 319–321.

[32] M. Bennett and K. Wiesenfeld (unpublished).

[33] N. Stocks, *Suprathreshold stochastic resonance in multilevel threshold systems*, *Phys. Rev. Lett.* **84** (2000) 2310–2313.

[34] D. Allingham, N. Stocks and R. Morse, *Use of suprathreshold stochastic resonance in cochlear implant coding*, in Proc. of the SPIE – The International Society for Optical Engineering, **5110** (2003) 92–101.